Supplemental Information for “The Anthropocene by the Numbers: A Quantitative Snapshot of Humanity’s Influence on the Planet”

Griffin Chure[1,a], Rachel A. Banks[2], Avi I. Flamholz[2], Nicholas S. Sarai[3], Mason Kamb[4], Ignacio Lopez-Gomez[5], Yinon M. Bar-On[6], Ron Milo[6], Rob Phillips[2,4,7,*]

[1]Department of Applied Physics and Materials Science, California Institute of Technology, Pasadena, CA, USA
[2]Division of Biology and Biological Engineering, California Institute of Technology, Pasadena, CA, USA
[3]Division of Chemistry and Chemical Engineering, California Institute of Technology, Pasadena, CA, USA
[4]Chan-Zuckerberg BioHub, San Francisco, CA, USA
[5]Department of Environmental Science and Engineering, California Institute of Technology, Pasadena, CA, USA
[6]Department of Plant and Environmental Sciences, Weizmann Institute of Science, Rehovot, Israel
[7]Department of Physics, California Institute of Technology, Pasadena, CA, USA

[a]Current Address: Department of Biology, Stanford University, Stanford, CA, USA

SI Section 1: References and Explanations For Values Reported in Figure 1

In this section, we report our extensive and detailed referencing for each and every quantity reported in the subpanels of Figure 1 of the main text. As described in the Materials & Methods, each value comes from the manual curation of a piece of scientific, industrial, governmental, or non-governmental organization reports, articles, or databases. Each value listed here contains information about the original source, the method used to obtain the value, as well as accession identification numbers for the Human Impacts Database (https://anthroponumbers.org), listed as HuIDs.

For each value, we attempt to provide an assessment of the uncertainty. For some values, this corresponds to the uncertainty in the measurement or inference as stated in the source material. In cases where a direct assessment of the uncertainty was not clearly presented, we sought other reported values for the same quantity from different data sources to present a range of the values. For others, this uncertainty represents the upper- and lower-bounds of the measurement or estimation.

Each value reported here is prefixed with a symbol representing our confidence in the value. Cases in which an equality (=) symbol is used represents that a measure of the uncertainty is reported in the original data source or represents a range of values from different sources that are tightly constrained (with 2 significant digits). An approximation symbol (≈) indicates values that we are confident in to within a factor of a few. In some cases, an approximation symbol (≈) represents a range where the values from different sources differ within three significant digits. In these cases, the ranges are presented as well. Finally, in some cases only a lower-bound for the quantity was able to be determined. These values are indicated by the use of an inequality symbol (>),.

A. SURFACE WARMING

Surface temperature change from the 1850-1900 average ≈ 1.0 - 1.4 °C (HuID: 79598, 76539, 12147)

Data Source(s): HadCRUT.4.6 (Morice et al., 2012, DOI: 10.1029/2011JD017187), GISTEMP v4 (GISTEMP Team, 2020: GISS Surface Temperature Analysis (GISTEMP), version 4. NASA Goddard Institute for Space Studies. Dataset accessed 2020-12-17 at https://data.giss.nasa.gov/gistemp/ & Lenssen et al., 2019, DOI: 10.1029/2018JD029522) and NOAAGlobalTemp v5 (Zhang et al, 2019, DOI: 10.1029/2019EO128229) datasets.

Notes: The global mean surface temperature captures near-surface air temperature over the planet’s land and ocean surface. The value reported represents the spread of three estimates and their 95% confidence intervals.Since data for the period 1850-1880 are missing in GISTEMP v4 and NOAAGlobalTemp v5, data are centered by setting the 1880-1900 mean of all datasets to the HadCRUT.4.6 mean over the same period.

B. Annual Ice Melt

Glaciers = (3.0 ± 1.2) × 10^{11} m^3 / yr (HuID: 32459)

Data Sources: Intergovernmental Panel on Climate Change (IPCC) 2019 Special Report on the Ocean and Cryosphere in a Changing Climate. Table 2.A.1 on pp. 199-202.

Notes: Value corresponds to the trend of annual glacial ice volume loss (reported as ice mass loss) from major glacierized regions (2006-2015) based on aggregation of observation methods (original data source: Zemp et al. 2019, DOI:10.1038/s41586-019-1071-0) with satellite gravimetric observations (original data source: Wouters et al. 2019, DOI:10.3389/feart.2019.00096). Ice volume loss was calculated from ice mass loss assuming a standard pure ice density of 920 kg / m^3. Uncertainty represents a 95% confidence interval calculated from standard error propagation of the 95% confidence intervals reported in the original sources assuming them to be independent.

Ice sheets = (4.7 ± 0.4) × 10^{11} m^3 / yr (HuIDs: 95798; 93137)

Data Source(s): D. N. Wiese et al. 2019 JPL GRACE and GRACE-FO Mascon Ocean, Ice, and Hydrology Equivalent HDR Water Height RL06M CRI Filtered Version 2.0, Ver. 2.0, PO.DAAC, CA, USA. Dataset accessed [2020-Aug-10]. DOI: 10.5067/TEM- SC-3MJ62

Notes: Value corresponds to the trends of combined annual ice volume loss (reported as ice mass loss) from the Greenland and Antarctic Ice Sheets (2002-2020) measured by satellite gravimetry. Ice volume loss was calculated from ice mass loss assuming a standard pure ice density of 920 kg / m^3. Uncertainty represents one standard deviation and considers only propagation of monthly uncertainties in measurement.

Arctic sea ice = (3.0 ± 1.0) × 10^{11} m^3 / yr (HuID: 89520)

Data Source(s): PIOMAS Arctic Sea Ice Volume Reanalysis, Figure 1 of webpage as of October 31, 2020. Original method source: Schweiger et al. 2011, DOI:10.1029/2011JC007084

Notes: Value reported corresponds to the trend of annual volume loss from Arctic sea ice (1979-2020). The uncertainty in the trend represents the range in trends calculated from three ice volume determination methods.

C. Sea Ice Extent

Extent of loss at yearly maximum cover (September) ≈ 8.4 × 10^{10} m^2 / yr (HuID: 33993)

Extent loss at yearly minimum cover (March) ≈ 4.0 × 10^{10} m^2 / yr (HuID: 87741)

Average annual extent loss = 5.5 ± 0.2 × 10^{10} m^2 / yr (HuID: 70818)

Data Source(s): Comiso et al. 2017, DOI:10.1002/2017JC012768. Fetterer et al. 2017, updated daily. Sea Ice Index, Version 3, Boulder, Colorado USA. NSIDC: National Snow and Ice Data Center, DOI:10.7265/N5K072F8, [Accessed 2020-Oct-19].

Notes: Sea ice extent refers to the area of the sea with > 15% ice coverage. Annual value corresponds to the linear trend of annually averaged Arctic sea ice extent from 1979-2015 (Comiso et al. 2017) calculated from four different methods. This is in good agreement with the linear trend of annual extent loss calculated by averaging over every month in a given year (5.5 × 10^{10} m^2 / yr HuID: 66277). The minimum cover extent loss corresponds to the linear trend of Arctic sea ice extent in September from 1979-2020 and the maximum cover extent loss corresponds to the linear trend of sea ice extent in March from 1979-2020. The Antarctic sea ice extent trend is not shown because a significant long-term trend over the satellite observation period is not observed and short-term trends are not yet identifiable.

D. Annual Material Production

Concrete production ≈ (2 - 3) × 10^{13} kg / yr (HuID: 25488; 81346; 16995)

Data Source(s): United States Geological Survey (USGS), Mineral Commodity Summaries 2020, pp. 42-43, DOI:10.3133/mcs2020. Miller et al. 2016, Table 1, DOI:10.1088/1748-9326/11/7/074029. Monteiro et al. 2017, DOI:10.1038/nmat4930. Krausmann et al. 2017, DOI:10.1073/pnas.1613773114

Notes: Concrete is formed when aggregate material is bonded together by hydrated cement. The USGS reports the mass of cement produced in 2019 as 4.1×10^{12} kg. As most cement is used to form concrete, cement production can be used to estimate concrete mass using a multiplicative conversion factor of 7 (Monteiro et al.). Miller et al. report that the cement, aggregate and water used in concrete in 2012 sum to 2.3×10^{13} kg. Krausmann et al. report an estimated value from 2010 based on a material input, stocks, and outputs model. The value is net annual addition to concrete stocks plus annual waste and recycling to estimate gross production of concrete.

Steel production = $(1.4 - 1.9) \times 10^{12}$ kg / yr (HuID: 51453; 44894; 85981)

Data Source(s): United States Geological Survey (USGS), Mineral Commodity Summaries 2020, pp. 82-83, DOI:10.3133/mcs2020. World Steel Association, World Steel in Figures 2020, p. 6. Krausmann et al. 2017, DOI:10.1073/pnas.1613773114

Notes: Crude steel includes stainless steels, carbon steels, and other alloys. The USGS reports the mass of crude steel produced in 2019 as 1900 megatonnes (Mt). The World Steel Association reports a production value of 1869 Mt in 2019. Krausmann et al. report an estimated value from 2010 based on a material input, stocks, and outputs model. The value is net annual addition to steel stocks plus annual waste and recycling to estimate gross production of steel.

Plastic production ≈ 4×10^{11} kg / yr (HuID: 97241; 25437)

Data Source(s): Geyer et al. 2017, Table S1, DOI:10.1126/sciadv.1700782. Krausmann et al. 2017, DOI:10.1073/pnas.1613773114

Notes: Value represents the approximate sum total global production of plastic fibers and plastic resin during the calendar year of 2015. Comprehensive data about global plastic production is sorely lacking. Geyer et al. draw data from various industry groups to estimate total production of different polymers and additives. Some of the underlying data is not publicly available, and data from financially-interested parties is inherently suspect. Krausmann et al. report an estimated value from 2010 based on a material input, stocks, and outputs model. The value is net annual addition to stocks plus annual waste and end-of-life recycling to estimate gross production of plastics.

E. Livestock Population

Chicken standing population ≈ 2.5×10^{10} (HuID: 94934)
Cattle standing population ≈ 1.5×10^{9} (HuID: 92006)
Swine standing population ≈ 1×10^{9} (HuID: 21368)
All livestock standing population ≈ 3×10^{10} (HuID: 43599)

Data Source(s): Food and Agriculture Organization (FAO) of the United Nations Statistical Database (2020) — Live Animals.

Notes: Counts correspond to the estimated standing populations in 2018. Values are reported directly by countries. The FAO uses non-governmental statistical sources to address uncertainty and missing (non-reported) data. Reported values are therefore approximations.

F. Annual Synthetic Nitrogen Fixation

Annual mass of synthetically fixed nitrogen ≈ 1.5×10^{11} kg N / yr (HuID: 60580; 61614)

Data Source(s): United States Geological Survey (USGS), Mineral Commodity Summaries 2020, pp. 116-117, DOI:10.3133/mcs2020. International Fertilizer Association (IFA) Statistical Database (2020) — Ammonia Production & Trade Tables by Region. Smith et al. 2020, DOI: 10.1039/c9ee02873k.

Notes: Ammonia (NH_3) produced globally is compiled by the USGS and IFA from major factories that report output. The USGS estimates the approximate mass of nitrogen in ammonia produced in 2018 as 1.50×10^{11} kg N and the International Fertilizer Association reports a production value of 1.50×10^{11} kg N in 2019. Nearly all of this mass is produced by the Haber-Bosch process (>96%, Smith et al. 2020). In the United States most of this mass is used for fertilizer, with the remainder being used to synthesize nitrogen-containing chemicals including explosives, plastics, and pharmaceuticals (≈ 88%, USGS Mineral Commodity Summaries 2020).

G. Ocean Acidity

Surface ocean [H+] ≈ 0.2 parts per billion (HuID: 90472)

Annual change in [H+] = *0.36 ± 0.03% (HuID: 19394)*

Data Source(s): Figures 1-2 of European Environment Agency report CLIM 043 (2020). Original data source of the report is "Global Mean Sea Water pH" from Copernicus Marine Environment Monitoring Service.

Notes: Reported value is calculated from the global average annual change in pH over years 1985-2018. The average oceanic surface pH was ≈ 8.057 in 2018 and decreases annually by ≈ 0.002 units, giving a change in [H+] of roughly $10^{-8.055}$ - $10^{-8.057}$ ≈ 4×10^{-11} mol/L or about 0.4% of the global average. [H+] is calculated as 10^{-pH} ≈ 10^{-8} mol/L or 0.2 parts per billion (ppb), noting that [H_2O] ≈ 55 mol/L. Uncertainty for annual change is the standard error of the mean.

H. Land Use

Agriculture ≈ 5 × 10^{13} m^2 (HuID: 29582)

Data Source(s): Food and Agriculture Organization (FAO) of the United Nations Statistical Database (2020) — Land Use.

Notes: Agricultural land is defined as all land that is under agricultural management including pastures, meadows, permanent crops, temporary crops, land under fallow, and land under agricultural structures (such as barns). Reported value corresponds to 2017 estimates by the FAO.

Urban ≈ (6 - 8) × 10^{11} m^2 (HuID: 41339; 39341)

Data Source(s): Florczyk et al. 2019 (https://tinyurl.com/yyxxgtll) and Table 3 of Liu et al. 2018 DOI: 10.1016/j.rse.2018.02.055

Notes: Urban land area is determined from satellite imagery. An area is determined to be "urban" if the total population is greater than 5,000 and has a minimum population density of 300 people per km^2. Reported value gives the range of recent measurements of ≈ 6.5×10^{11} m^2 (2015) and ≈ (7.5 ± 1.5) $\times 10^{11}$ m^2 (2010) from Florczyk et al. 2019 and Liu et al. 2018, respectively.

I. River Fragmentation

Global fragmented river volume ≈ 6 × 10^{11} m^3 (HuID: 61661)

Data Source(s): Grill et al. 2019 DOI: 10.1038/s41586-019-1111-9

Notes: Value corresponds to the water volume contained in rivers that fall below the connectivity threshold required to classify them as free-flowing. Value considers only rivers with upstream catchment areas greater than 10 km^2 or discharge volumes greater than 0.1 m^3 per second. The ratio of global river volume in disrupted rivers to free-flowing rivers is approximately 0.9. The exact value depends on the cutoff used to define a "free-flowing" river. We direct the reader to the source for thorough detail.

J. Human Population

Urban population ≈ 55% (HuID: 93995)

Global population ≈ 7.6 × 10^9 people (HuID: 85255)

Data Source(s): Food and Agricultural Organization (FAO) of the United Nations Report on Annual Population, 2019.

Notes: Value for total population in 2018 comes from a combination of direct population reports from country governments as well as inferences of underreported or missing data. The definition of "urban" differs between countries and the data does not distinguish between urban and suburban populations despite substantive differences between these land uses (Jones & Kammen 2013, DOI: 10.1021/es4034364). As explained by the United Nations population division, "When the definition used in the latest census was not the same as in previous censuses, the data were adjusted whenever possible so as to maintain consistency." Rural population is computed from this fraction along with the total human population, implying that the total population is composed only of “urban” and “rural” communities.

K. Greenhouse Gas Emissions

Anthropogenic CO_2 = $(4.25 \pm 0.33) \times 10^{13}$ kg CO_2 / yr (HuID: 24789; 54608; 98043; 60670)

Data Source(s): Table 6 of Friedlingstein et al. 2019, DOI: 10.5194/essd-11-1783-2019. Original data sources relevant to this study compiled in Friedlingstein et al.: 1) Gilfillan et al. https://energy.appstate.edu/CDIAC 2) Average of two bookkeeping models: Houghton and Nassikas 2017 DOI: 10.1002/2016GB005546; Hansis et al. 2015 DOI: 10.1002/2014GB004997. 3) Dlugokencky and Tans, National Oceanic & Atmospheric Administration, Earth System Research Laboratory (NOAA/ESRL), https://www.esrl.noaa.gov/gmd/ccgg/trends/global.html, [Accessed 3-Nov-2019].

Notes: Value corresponds to total CO_2 emissions from fossil fuel combustion, industry (predominantly cement production), and land-use change during calendar year 2018. Emissions from land-use change are due to the burning or degradation of plant biomass. In 2018, roughly 1.88×10^{13} kg CO_2 / yr accumulated in the atmosphere, reflecting the balance of emissions and CO_2 uptake by plants and oceans (Dlugokencky and Tans). Uncertainty corresponds to one standard deviation.

Anthropogenic CH_4 = $(3.4 - 3.9) \times 10^{11}$ kg CH_4 / yr (HuID: 96837; 30725)

Data Source(s): Table 3 of Saunois, et al. 2020. DOI: 10.5194/essd-12-1561-2020.

Notes: Value corresponds to 2008-2017 decadal average mass of CH_4 emissions from anthropogenic sources. Includes emissions from agriculture and landfill, fossil fuels, and burning of biomass and biofuels, but other inventories of anthropogenic methane emissions are also considered. Reported range represents the minimum and maximum estimated emissions from a combination of “bottom-up” and “top-down” models.

Anthropogenic N_2O = $1.1\ (+0.6, -0.5) \times 10^{10}$ kg N_2O / yr (HuID: 44575)

Data Source(s): Table 1 of Tian, H., et al. 2020. DOI: 10.1038/s41586-020-2780-0

Notes: Value corresponds to annualized N_2O emissions from anthropogenic sources in the years 2007-2016. The value reported in the source is 7.3 [4.2, 11.4] Tg N / year. This is converted to a mass of N_2O using the fact that N ≈ 14/22 of the mass of N_2O. Reported value is mean with the uncertainty bounds (+,-) representing the maximum and minimum values observed in the 2007-2016 time period.

L. Water Withdrawal

Agricultural = 1.3×10^{12} m^3 / year (HuID: 84545, 43593, 95345)
Industrial = 5.9×10^{11} m^3 / year (HuID: 27142)
Domestic = 5.4×10^{10} m^3 / year (HuID: 69424)
Total = $(1.7 - 2.2) \times 10^{12}$ m^3 / year (HuID: 27342, 68004)

Data Source(s): Figure 1 of Qin et al. 2019. DOI: 10.1038/s41893-019-0294-2. AQUASTAT Main Database, Food and Agriculture Organization of the United Nations

Notes: “Agricultural” and “total” withdrawal include one value from Qin et al. (who reports “consumption”) and one value from the AQUASTAT database. Industrial water withdrawal is from AQUASTAT and domestic withdrawal value is from Qin et al. Values in AQUASTAT are self-reported by countries and have missing values from some countries, probably accounting for a few percent underreporting. All values represent water withdrawals. For agricultural and domestic, water withdrawal is assumed to be the same as water consumption, which is reported in Qin et al.

M. Sea Level Rise

Added water = 1.97 (+0.36, -0.34) mm / yr (HuID: 97108)

Thermal expansion = 1.19 (+0.25, -0.24) mm / yr (HuID: 97688)
Total observed sea-level rise = 3.35 (+0.47, -0.44) mm / yr (HuID: 81373)
Data Source(s): Table 1 of Frederikse et al. 2020. DOI:10.1038/s41586-020-2591-3.
Notes: Values correspond to the average global sea level rise for the years 1993 - 2018. "Added water" (barystatic) change includes effects from meltwater from glaciers and ice sheets, added mass from sea-ice discharge, and changes in the amount of terrestrial water storage. Thermal expansion accounts for the volume change of water with increasing temperature. Values for "thermal expansion" and "added water" come from direct observations of ocean temperature and gravimetry/altimetry, respectively. Total sea level rise is the observed value using a combination of measurement methods. "Other sources" reported in Figure 1 accounts for observed residual sea level rise not attributed to a source in the model. Values in brackets correspond to the upper and lower bounds of the 90% confidence interval.

N. Total Power Use

Global power use ≈ 19 - 20 TW (HuID: 31373; 85317)
Data Source(s): bp Statistical Review of World Energy, 2020; U.S. Energy Information Administration, 2020.
Notes: Value represents the sum of total primary energy consumed from oil, natural gas, coal, and nuclear energy and electricity generated by hydroelectric and other renewables. Value is calculated using annual primary energy consumption as reported in data sources assuming uniform use throughout a year, yielding ≈ 19 - 20 TW.

O. Tree Coverage Area Loss

Commodity-driven deforestation = (5.7 ± 1.1) × 10^{10} m^2 / yr (HuID: 96098)
Forestry = (5.4 ± 0.8) × 10^{10} m^2 / yr (HuID: 38352)
Urbanization = (2 ± 1) × 10^9 m^2 / yr (HuID: 19429)
Shifting agriculture = (7.5 ± 0.9) × 10^{10} m^2 / yr (HuID: 24388)
Wildfire = (7.2 ± 1.3) × 10^{10} m^2 / yr (HuID: 92221)
Total tree cover area loss ≈ 2 × 10^{11} m^2 / yr (HuID: 78576)
Data Source(s): Table 1 of Curtis et al. 2018 DOI:10.1126/science.aau3445. Hansen et al. 2013 DOI:10.1126/science.1244693. Global Forest Watch, 2020. Reported values in source correspond to total loss from 2001 - 2015. Values given are averages over this 15 year window.
Notes: Commodity-driven deforestation is "long-term, permanent, conversion of forest and shrubland to a non-forest land use such as agriculture, mining, or energy infrastructure." Forestry is defined as large-scale operations occurring within managed forests and tree plantations with evidence of forest regrowth in subsequent years. Urbanization converts forest and shrubland for the expansion and intensification of existing urban centers. Disruption due to "shifting agriculture" is defined as "small- to medium-scale forest and shrubland conversion for agriculture that is later abandoned and followed by subsequent forest regrowth". Disruption due to wildfire is "large-scale forest loss resulting from the burning of forest vegetation with no visible human conversion or agricultural activity afterward." Uncertainty corresponds to the reported 95% confidence interval. Uncertainty is approximate for "urbanization" as the source reports an ambiguous error of "± <1%."

P. Power From Fossil Fuels

Natural gas = 4.5 - 4.8 TW (HuID: 49947; 86175)
Oil = 6.1 - 6.6 TW (HuID: 42121; 39756)
Coal = 5.0 - 5.5 TW (HuID: 10400; 60490)
Total = 16 - 17.0 TW (HuID: 29470; 29109)
Data Source(s): bp Statistical Review of World Energy, 2020. U.S. Energy Information Administration, 2020.
Notes: Values are self-reported by countries. All values from bp Statistical Review correspond to 2019 whereas values from the EIA correspond to 2018 estimates. Reported TW values are computed from primary energy units (e.g. kg coal) assuming uniform use throughout the year. Oil volume includes crude oil, shale oil, oil sands,

condensates, and natural gas liquids separate from specific natural gas mining. Natural gas value excludes gas flared or recycled and includes natural gas produced for gas-to-liquids transformation. Coal value includes 2019 value exclusively for solid commercial fuels such as bituminous coal and anthracite, lignite and subbituminous coal, and other solid fuels. This includes coal used directly in power production as well as coal used in coal-to-liquids and coal-to-gas transformations.

Q. Power From Renewable Resources

Wind = 0.36 - 0.39 TW (HuID: 30581, 85919)
Solar = 0.18 - 0.20TW (HuID: 99885, 58303)
Hydroelectric = 1.2 - 1.3 TW (HuID: 15765, 50558)
Total = 1.9 - 2.1 TW (HuID: 74571, 20246)

Data Source(s): bp Statistical Review of World Energy, 2020. U.S. Energy Information Administration, 2020.
Notes: Reported values correspond to estimates for the 2019 calendar year for BP and 2018 for EIA data, except for total renewables, which is from 2017. Renewable resources are defined as wind, geothermal, solar, biomass and waste. Hydroelectric, while presented here, is not defined as a renewable in the BP dataset. All values are reported as input-equivalent energy, meaning the input energy that would have been required if the power was produced by fossil fuels. BP reports that fossil fuel efficiency used to make this conversion was about 40% in 2017.

R. Fossil Fuel Extraction

Natural gas volume = (3.9 - 4.0) × 10^{12} m^3 / yr (HuID: 11468; 20532)
Oil volume = (5.5 - 5.8) × 10^9 m^3 / yr (HuID: 66789; 97719)
Coal mass = (7.8 - 8.1) × 10^{12} kg / yr (HuID: 78435; 48928)

Data Source(s): bp Statistical Review of World Energy, 2020. U.S. Energy Information Administration (EIA), 2020.
Notes: Oil volume includes crude oil, shale oil, oil sands, condensates, and natural gas liquids separate from specific natural gas mining. Natural gas value excludes gas flared or recycled and includes natural gas produced for gas-to-liquids transformation. Coal value includes solid commercial fuels such as bituminous coal, anthracite, lignite, subbituminous coal, and other solid fuels. All values from bp Statistical Review correspond to 2019 whereas values from the EIA correspond to 2018 estimates.

S. Ocean Warming

Heat uptake = $346 \pm 51\ TW$ *(HuID: 94108)*
Upper ocean (0 - 700m) temperature increase since to 1960 = $0.18 - 0.20$ ℃ *(HuID: 69674, 72086)*

Data Source(s): Table S1 of Cheng et al. 2017. DOI: 10.1126/sciadv.1601545. NOAA National Centers for Environmental Information, 2020. DOI: 10.1029/2012GL051106.
Notes: Heat uptake reported is the average over time period 1992-2015 with 95% confidence intervals. Range of temperatures reported captures the 95% confidence interval of temperature increase for the period 2015-2019 with respect to the 1958-1962 mean. Temperature change is considered in the upper 700 m because sea surface temperatures have high decadal variability and are a poor indicator of ocean warming; see Roemmich et al. 2015, DOI: 10.1038/NCLIMATE2513.

T. Power From Nuclear Fission

Nuclear power ≈ 0.79 - 0.89 TW (HuID: 48387; 71725)

Data Source(s): bp Statistical Review of World Energy, 2020. U.S. Energy Information Administration (EIA), 2020
Notes: Values are self-reported by countries and correspond to estimates for the 2019 calendar year from BP and 2018 from EIA. Values are reported as ‘input-equivalent’ energy, meaning the energy that would have been needed to produce a given amount of power if the input were a fossil fuel, which is converted to TW here. This is calculated by multiplying the given power by a conversion factor representing the efficiency of power production by fossil fuels. In 2017, this factor was about 40%.

U. Nuclear Fallout

Anthropogenic ^{239}Pu and ^{240}Pu from nuclear weapons ≈ 1.4 $\times$ 10^{11} kg / yr (HuID: 42526)
Data Source(s): Table 1 in Hancock et al. 2014 doi: 10.1144/SP395.15. Fallout in activity from UNSCEAR 2000 Report on Sources and Effects of Ionizing Radiation Report to the UN General Assembly -- Volume 1.
Notes: The approximate mass of Plutonium isotopes ^{239}Pu and ^{240}Pu released into the atmosphere from the ≈ 500 above-ground nuclear weapons tests conducted between 1945 and 1980. Naturally occurring ^{239}Pu and ^{240}Pu are rare, meaning that nearly all contemporary labile plutonium comes from human production (Taylor 2001,doi: 10.1016/S1569-4860(01)80003-6). The total mass of radionuclides released is ≈ 3300 kg with a combined radioactive fallout of ≈ 11 PBq. These values do not represent the entire 239+240Pu globally distributed mass as it excludes non-weapons sources.

V. Contemporary Extinction

Animal species extinct since 1500 > 750 (HuID: 44641)
Plant species extinct since 1500 > 120 (HuID: 86866)
Data Source(s): The IUCN Red List of Threatened Species. Version 2020-2
Notes: Values correspond to absolute lower-bound count of animal extinctions over the past ≈ 520 years. Of the predicted ≈ 8 million animal species, the IUCN databases catalogues only ≈ 900,000 with only ≈ 75,000 being assigned a conservation status. Representation of plants and fungi is even more sparse with only ≈ 40,000 and ≈ 285 being assigned a conservation status, respectively. The number of extinct animal species is undoubtedly higher than these reported values, as signified by an inequality symbol (>).

W. Earth Moving

Waste and overburden from coal mining ≈ 6.5 × 10^{13} kg / yr (HuID: 72899)
Earth moved from urbanization > 1.4 × 10^{14} kg / yr (HuID: 59640)
Data Source(s): Supplementary table 1 of Cooper et al. 2018. DOI: doi.org/gfwfhd.
Notes: Coal mining waste and overburden mass is calculated given commodity-level stripping ratios (mass of overburden/waste per mass of coal resource mined) and reported values of global coal production by type. Urbanization mass is presented as a lower bound estimate of the mass of earth moved from global construction projects. This comes from a conservative estimate that the ratio of the mass of earth moved per mass of cement/concrete used in construction globally is 2:1. This value is highly context dependent and we encourage the reader to read the source material for a more thorough description of this estimation.
Erosion rate from agriculture > (1.2 - 2.4) × 10^{13} kg / yr (HuID: 19415; 41496)
Data Source(s): Pg. 377 of Wang and Van Oost 2019. DOI: 10.1177/0959683618816499. Pg. 21996 of Borrelli et al. 2020 DOI: 10.1073/pnas.2001403117.
Notes: Cumulative sediment mass loss over history of human agriculture due to accelerated erosion is estimated to be ≈ 30,000 Gt. Recent years have an estimated erosion rate ranging from 12 Pg / yr (Wang and Van Oost) to ≈ 24 Pg / yr (Borrelli et al.). Values come from computational models conditioned on time-resolved measurements of sediment deposition in catchment basins.

SI Section 2: Connections Between Panels in Figure 1

In the main text, we presented a few examples of connections between the values displayed in Figure 1 could be drawn. Another way to approach these values is to begin with the question "how much water do we use?" A vast majority of human water use is for agriculture and industrial use (including cooling power plants, Figure 1 K; HuID: 84545, 43593, 95345; 27142). In order to harness this water, about half of the world's river volume is now under human control (Figure 1 H; HuID: 61661). Agricultural water use is mainly for irrigation of crops; approximately 10% of the total agricultural land area is irrigated (≈ 5 × 10^{12} m^2). These crops also require nitrogenous fertilizer to grow, requiring synthetic fixation of nitrogen (Figure 1 E; HuID: 60580, 61614). Nitrogen fixation as well as rice paddies and livestock are major sources of N_2O and CH_4 emissions (Figure 1 J; HuID: 96837, 30725; 44575). Another major use of water by humans is for cooling power plants that generate power from fossil fuels (Figure 1 O; HuID: 29470, 29109). Generating this power requires extraction of massive amounts of coal, oil, and natural gas (Figure 1 Q; HuID: 11468, 20532; 66789, 97719; 78435, 48928) and the movement of large amounts of geological materials (Figure 1 V; HuID: 72899).

SI Section 3: Region Definitions

See the supplemental file "region definitions" for a list of countries and their associated regions used in this study. For tree cover area loss, we did not have access to data at the country level and used slightly different region definitions: Central & South America; North America; Russia, China & South Asia; Southeast Asia; Europe (except Russia); Africa; and Oceania

SI Section 4: Discussion of Regional Distributions

While Figure 1 presents the magnitude of human impacts at a global scale, it is important to recognize that these human impacts — both their origins and repercussions — are highly variable across the globe. The distribution of the global population and the societal and cultural differences which prescribe our interactions with the planet lead to unequal contributions to these impacts featured in Figure 1. The outcomes of these impacts are also unequally distributed, leading to some regions being disproportionately affected by the consequences of human activities. Figure S1 displays a coarse regional breakdown of the numbers from Figure 1 for which regional distributions could be determined. The region definitions used in Figure S1 are similar to the definitions set forth by the Food and Agricultural Organization (FAO) of the United Nations, assigning the semi-continental regions of North America, South America, Africa, Europe, Asia, and Oceania. Supplementary Information Section 3 provides a list of the defined regions along with the countries and localities which form them. Here, we specify both the total contribution of each region and the per capita value given the population of that region at the year(s) in which the quantity was measured. While we have chosen here to present a somewhat simplistic regional breakdown, there are many possible ways to look at the data, such as by country or regional economic activity. We hope this resource inspires others to examine these data with different regional definitions.

Much as in the case of Figure 1, interesting details emerge naturally from the display of the data shown in Figure S1. For example, Asia dominates global agricultural water withdrawal, using about 62%, while Northern America takes the lead for industrial water withdrawal, much of which is used for the production of electricity. From considering the volume of water withdrawn per capita, however, we find that Northern America withdraws more water per person than any other region for agricultural, industrial, and domestic water use.

Northern America also emits far more CO_2 per person than any other region, with Oceania and Europe coming second and third, respectively. This disparity can be partially understood by considering how each region uses nuclear fission, fossil fuel combustion, and renewable resources as sources of energy. While Asia consumes half of total power, per capita consumption is markedly lower than North America, Europe, and Oceania due to Asia having more than fivefold greater population than those other regions. Interestingly, renewables and nuclear power tell a different story. Southern America, while consuming merely 4% of total power, generates about 14% of renewable energy. Nuclear power generation, on the other hand, is dominated by Northern America and Europe, while Oceania, which has only a single research-grade nuclear reactor, comes dead last.

Investigating forest loss by region and cause provides a clearer picture of the contemporary trends. At a global level, all drivers of forest loss are comparable in magnitude except for urbanization, which is responsible for ≈ 1% of total tree cover area loss. However, when each driver is broken down by region, it becomes apparent that not all regions are comparable. Central and South America account for 64% of commodity-driven deforestation (meaning, clearcutting with no substantial regrowth of tree cover), whereas a majority of forest loss due to shifting agriculture occurs in Africa (where regrowth does occur). Together, wildfires in North America, Russia, China, and South Asia make up nearly 90% of the fire-based loss in tree cover. North America alone, which has had periodic and enormous wildfires over the past two decades, accounts for around 42% of fire-based loss. Finally, urbanization is dominated by development in South Asia. It is important to realize that while urbanization at a global level is the smallest driver of tree cover loss, it can still have strong impacts at the regional level, greatly perturbing local ecosystems and biodiversity.

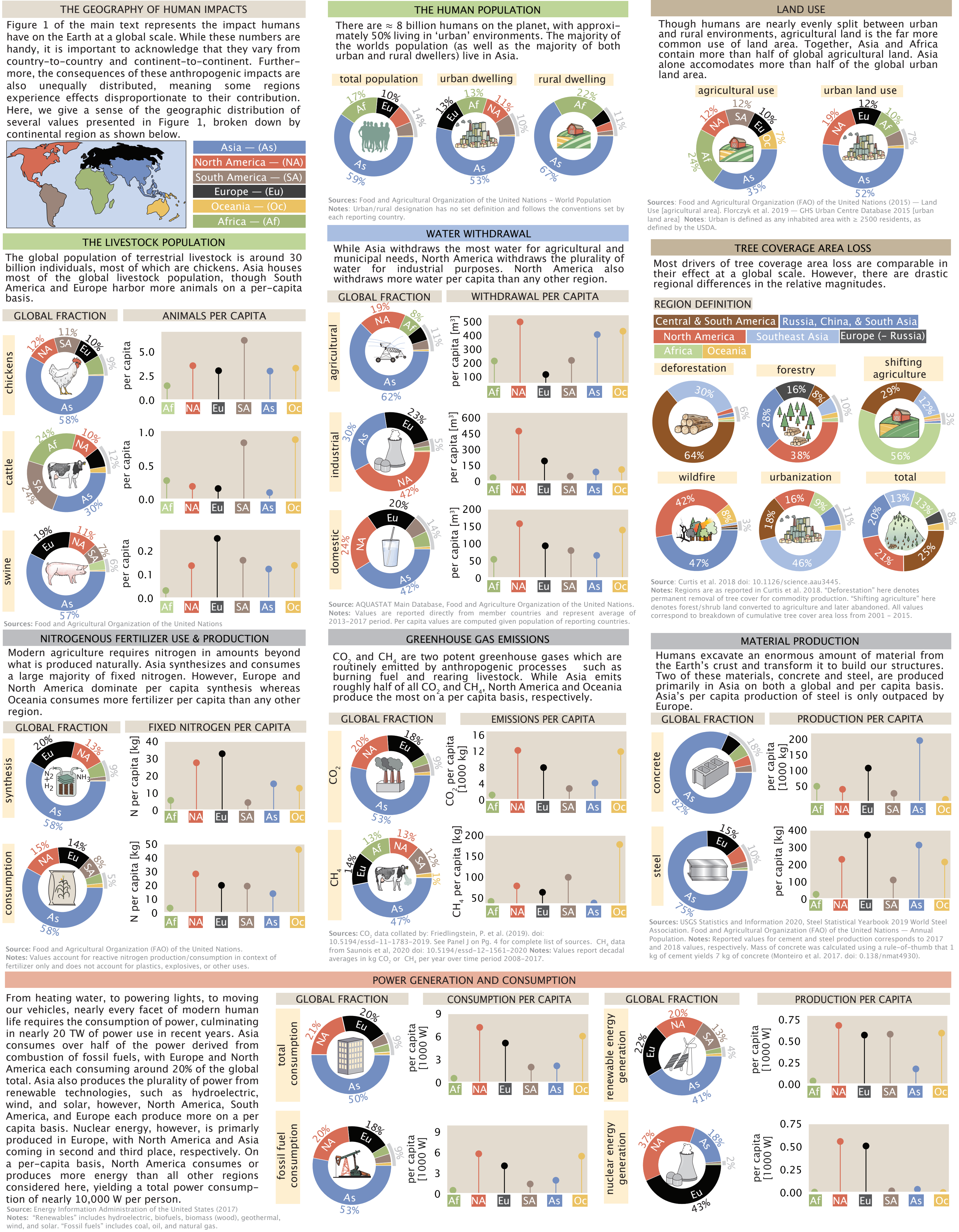

Figure S1: The regional distribution of human impacts on the planet. A subset of the quantities presented in Figure 1 are shown here broken down by geographic region. Unless otherwise noted, regions follow the Food and Agricultural Organization delineations of world regions, with the Caribbean subsumed into output for Northern America.